

Is Meta-Path Attention an Explanation? Evidence of Alignment and Decoupling in Heterogeneous GNNs

Maiqi Jiang

William & Mary

Williamsburg, Virginia, USA

mjiang04@wm.edu

Yiran Ding

Brown University

Providence, Rhode Island, USA

yiran_ding@alumni.brown.edu

Noman Ali

Indian Institute of Technology

Jodhpur, India

21f1004271@ds.study.iitm.ac.in

Yanfu Zhang*

William & Mary

Williamsburg, Virginia, USA

yzhang105@wm.edu

Abstract

Meta-path-based heterogeneous graph neural networks aggregate over meta-path-induced views, and their semantic-level attention over meta-path channels is widely used as a narrative for “which semantics matter.” We study this assumption empirically by asking: *when does meta-path attention reflect meta-path importance, and when can it decouple?* A key challenge is that most post-hoc GNN explainers are designed for homogeneous graphs, and naive adaptations to heterogeneous neighborhoods can mix semantics and confound perturbations. To enable a controlled empirical analysis, we introduce **MetaXplain**, a meta-path-aware post-hoc explanation protocol that applies existing explainers in the native meta-path view domain via (i) view-factorized explanations, (ii) schema-valid channel-wise perturbations, and (iii) fusion-aware attribution, without modifying the underlying predictor. We benchmark representative gradient-, perturbation-, and Shapley-style explainers on ACM, DBLP, and IMDB with HAN and HAN-GCN, comparing against XPath and type-matched random baselines under standard faithfulness metrics. To quantify attention reliability, we propose **Meta-Path Attention–Explanation Alignment (MP-AEA)**, which measures rank correlation between learned attention weights and explanation-derived meta-path contribution scores across random runs. Our results show that meta-path-aware explanations typically outperform random controls, while MP-AEA reveals both high-alignment and statistically significant decoupling regimes depending on the dataset and backbone; moreover, retraining on explanation-induced subgraphs often preserves, and in some noisy regimes improves, predictive performance, suggesting an explanation-as-denoising effect.

*Corresponding author.

Permission to make digital or hard copies of all or part of this work for personal or classroom use is granted without fee provided that copies are not made or distributed for profit or commercial advantage and that copies bear this notice and the full citation on the first page. Copyrights for components of this work owned by others than the author(s) must be honored. Abstracting with credit is permitted. To copy otherwise, or republish, to post on servers or to redistribute to lists, requires prior specific permission and/or a fee. Request permissions from permissions@acm.org.

KDD 2026, Jeju, South Korea

© 2026 Copyright held by the owner/author(s). Publication rights licensed to ACM.

ACM ISBN 978-1-4503-XXXX-X/2018/06

<https://doi.org/XXXXXXX.XXXXXXX>

CCS Concepts

- Computing methodologies → Machine learning; • Information systems → Data mining.

Keywords

Heterogeneous Graph Neural Networks, Meta-Path, Explainable AI, Attention mechanisms

ACM Reference Format:

Maiqi Jiang, Noman Ali, Yiran Ding, and Yanfu Zhang. 2026. Is Meta-Path Attention an Explanation? Evidence of Alignment and Decoupling in Heterogeneous GNNs. In *Proceedings of 32nd SIGKDD Conference on Knowledge Discovery and Data Mining, 2026 (KDD 2026)*. ACM, New York, NY, USA, 13 pages. <https://doi.org/XXXXXXX.XXXXXXX>

1 Introduction

Graph Neural Networks (GNNs) have demonstrated significant success in processing graph-structured data [5, 6, 8, 17], and heterogeneous GNNs (HeteroGNNs) extend this capability to heterogeneous graphs by incorporating the multi-typed nature of nodes and edges. Many HeteroGNNs, such as HAN [23] and MAGNN [7], utilize *meta-paths*, sequences of node and edge types that capture meaningful relationships within the network. These meta-paths serve as powerful tools for representing task-relevant semantics within the graph structure.

Exploration goal: when is meta-path attention explanatory? Meta-path-based HeteroGNNs are often interpreted through the lens of *semantic-level attention* over meta-path channels: for example, in HAN, the learned attention weights over meta-path views are frequently treated as a post-hoc explanation of “which semantics matter.” However, a growing literature in both NLP and graph learning shows that attention weights need not reflect feature importance [9, 16, 20]. This raises a basic but unresolved question for heterogeneous graph learning: Does semantic-level attention reliably track meta-path importance, and if not, when does it decouple? This paper treats that question as an empirical one.

Why existing explainers can mislead under heterogeneity. Post-hoc explainability for homogeneous-graph GNNs has advanced rapidly, with gradient-, perturbation-, and search-based methods that attribute predictions to nodes, edges, or features [1, 18, 22, 27, 28]. But directly applying these explainers to meta-path-based HeteroGNNs

is not straightforward: a common naive strategy collapses the heterogeneous neighborhood into a single graph and runs a homogeneous explainer. Such collapsing can (i) *collapse semantics* by mixing edges arising from different meta-path views into indistinguishable connectivity, (ii) *confound perturbations* because editing a shared structural element can simultaneously disrupt multiple semantic channels, and (iii) *distort attribution under fusion* because cross-meta-path aggregation can suppress or cancel contributions at the output even when a meta-path is locally important. As a result, both attention-based narratives and post-hoc explanations can be difficult to interpret at the meta-path (semantic-channel) level and may fail basic faithfulness checks.

A meta-path-consistent protocol for post-hoc explanation. To enable a controlled empirical study of meta-path importance and attention reliability, we introduce **MetaXplain**, a meta-path-aware post-hoc explainability protocol for meta-path-based HeteroGNNs. MetaXplain is not a new predictor; rather, it standardizes how existing explainers are applied in the native computation domain of meta-path-based models. The key idea is to treat the meta-path-induced local view set $\mathcal{G}(v) = \{G_v^{(m)}\}_{m \in \mathcal{M}}$ as the explanation domain, and to enforce three consistency conditions that prevent invalid conclusions: (i) *view-factorized* explanation objects indexed by meta-path views, (ii) *channel-wise, schema-valid* perturbations or masks restricted within each view, and (iii) *fusion-aware* attribution that summarizes meta-path contributions without collapsing semantics. This protocol “lifts” a broad class of homogeneous-graph explainers into meta-path-induced view spaces without modifying the underlying trained model.

Diagnostic: measuring attention-importance agreement across runs. To directly test whether semantic attention is a faithful proxy for meta-path importance, we propose **Meta-Path Attention-Explanation Alignment (MP-AEA)**, which quantifies the agreement between (i) a model’s semantic attention distribution over meta-paths and (ii) explanation-derived meta-path contribution scores. MP-AEA measures rank correlation between these two quantities across random runs, turning the qualitative question “is attention explanatory?” into a reproducible diagnostic.

Empirical study and key observations. We instantiate MetaXplain with representative explainers spanning gradient-based, perturbation-based, and Shapley-style families (Grad [18, 21], GNNExplainer [27], PGM-Explainer [22], GraphSVX [4], and GNNShap [1]), and benchmark on ACM, DBLP, and IMDB with HAN and HAN-GCN, comparing against xPath [11] and type-matched random baselines under standard faithfulness metrics. Across datasets and backbones, lifted explainers typically outperform random baselines, but performance and stability are backbone-dependent. Most importantly, MP-AEA reveals that semantic attention can be reliable in some settings yet statistically decoupled from meta-path importance in others. Finally, we find that retraining on explanation-induced subgraphs often preserves, and in noisy spectral regimes can improve predictive performance, suggesting an *explanation-as-denosing* effect.

Our contributions are primarily diagnostic and empirical:

- We introduce **MetaXplain**, a meta-path-consistent post-hoc explanation protocol that standardizes how diverse homogeneous-graph explainers can be applied in the meta-path view domain

(view-factorized explanations, schema-valid channel-wise perturbation, fusion-aware attribution).

- We propose **MP-AEA**, a diagnostic that measures whether semantic-level meta-path attention tracks explanation-derived meta-path contributions across random runs.
- Through experiments on ACM, DBLP, and IMDB with HAN/HAN-GCN, we report empirical findings that (i) meta-path-aware explainers improve over type-matched random baselines but can be backbone-sensitive, (ii) semantic attention can align with or decouple from meta-path importance depending on the dataset / backbone, and (iii) explanation-induced subgraphs can act as denoising and support effective retraining.

2 Related Work

Post-hoc explainability for homogeneous-graph GNNs. Post-hoc explainability for homogeneous GNNs spans (i) gradient/saliency attribution and CAM-style variants [3, 18, 19, 21], (ii) mask-optimization explainers such as GNNExplainer and PGExplainer [13, 27], (iii) probabilistic/causal approaches (e.g., PGM-Explainer) [22], and (iv) Shapley-style attribution (e.g., GraphSVX, GNNShap) [1, 4]. Most of these methods assume a single unlabeled edge space and a homogeneous neighborhood, so their explanation variables (masks, perturbations, players) are not directly aligned with the *semantic channel decomposition* induced by meta-path views in heterogeneous graphs. In this paper, our goal is not to propose a new homogeneous explainer, but to enable a controlled *empirical study* of meta-path importance by applying existing explainers in a meta-path-consistent way.

Explainability for heterogeneous graphs. Explainability for heterogeneous graphs is less mature and often model- or task-specific. PaGE-Link [30] explains link prediction via influential paths, while other work derives symbolic or causal criteria under heterogeneity constraints [10, 14, 25]. Most closely related, xPath [11] generates type-aware explainable paths for heterogeneous predictions. These approaches highlight the importance of respecting schema semantics, but they do not directly provide a standardized protocol for analyzing meta-path-based pipelines that explicitly operate on meta-path-induced views (e.g., HAN [23]). Our work is complementary: we focus on meta-path-based HeteroGNNs and provide a meta-path-aware post-hoc protocol that standardizes how diverse existing explainers can be applied to the meta-path view domain, enabling apples-to-apples comparisons and downstream diagnostics of semantic-channel importance.

Is attention explanatory? Diagnostics and reliability. Attention is frequently used as an explanation mechanism, yet in NLP it is neither necessary nor sufficient in general [9, 16], with follow-up work studying conditions under which attention aligns with feature importance [24]. Similar concerns have been raised for attention mechanisms in graph models [20]. Despite the prevalence of *semantic-level meta-path attention* in models such as HAN, there is limited systematic evidence on when such attention reliably reflects meta-path importance rather than acting as a convenient but potentially misleading narrative. Motivated by this gap, our paper contributes a simple diagnostic, **MP-AEA**, that measures attention-importance agreement across random runs using explanation-derived meta-path contribution scores. This diagnostic

supports our central exploration question: when does meta-path attention align with, or decouple from, meta-path importance?

3 Preliminaries

A **heterogeneous graph** models multiple node and/or edge types to capture complex real-world semantics. Formally, let a typed graph be denoted by $\mathcal{G} = (\mathcal{V}, \mathcal{E}, \mathcal{T}, \mathcal{R})$, where \mathcal{T} is the set of node types and \mathcal{R} is the set of relation (edge) types, with type mappings $\phi: \mathcal{V} \rightarrow \mathcal{T}$ and $\psi: \mathcal{E} \rightarrow \mathcal{R}$. The graph is heterogeneous if $|\mathcal{T}| > 1$ or $|\mathcal{R}| > 1$; otherwise, it is homogeneous.

A meta-path is a typed relation sequence defined on the schema, capturing a semantic pattern of connectivity. Formally, a meta-path m can be written as $m: t_1 \xrightarrow{r_1} t_2 \xrightarrow{r_2} \dots \xrightarrow{r_\ell} t_{\ell+1}$, where $t_i \in \mathcal{T}$ and $r_i \in \mathcal{R}$. Two nodes u and v are meta-path-connected by m if there exists an instance path in \mathcal{G} whose node/edge types match the sequence m .

Given a meta-path $m \in \mathcal{M}$, we denote the *meta-path-induced view* (or meta-path graph) as $G^{(m)} = (\mathcal{V}, \mathcal{E}^{(m)})$, where $(u, v) \in \mathcal{E}^{(m)}$ if u and v are connected by at least one instance path following m . This construction is widely used in meta-path-based heterogeneous learning to provide a semantic-specific neighborhood for aggregation.

For a target node v , we define its *local meta-path computation graphs* as

$$\mathcal{G}(v) = \{G_v^{(m)} \mid m \in \mathcal{M}\}, \quad (1)$$

where $G_v^{(m)}$ is typically an ego-subgraph (e.g., k -hop neighborhood) of v extracted from $G^{(m)}$. We treat $\mathcal{G}(v)$ as the native computation domain of meta-path-based models and, correspondingly, the native domain for post-hoc explanation in our study.

3.1 Meta-path-based HeteroGNN Interface

Many meta-path-based HeteroGNNs follow a two-stage computation: (i) *within-meta-path* aggregation to compute channel-wise embeddings and (ii) *cross-meta-path* fusion to produce the final representation and prediction. We abstract this family via the following interface:

$$\mathbf{h}_v^{(m)} = g^{(m)}(G_v^{(m)}, X), \quad \forall m \in \mathcal{M}, \quad (2)$$

$$f(v) = \text{Dec}(\mathbf{h}_v), \mathbf{h}_v = \text{Fuse}\left(\{\mathbf{h}_v^{(m)}\}_{m \in \mathcal{M}}\right), \quad (3)$$

where X denotes node features (optionally type-specific), $\text{Fuse}(\cdot)$ is a semantic fusion operator, and $\text{Dec}(\cdot)$ is a task head. For instance, HAN [23] realizes $\text{Fuse}(\cdot)$ with semantic-level attention over meta-path channels, while SeHGNN [26] uses a simplified neighbor aggregation with a semantic fusion module (e.g., transformer-style fusion) over meta-path-derived representations.

3.2 Post-hoc Explainability Setup

We focus on *post-hoc* explanation: given a trained predictor f and a specific prediction for target v , the goal is to output an explanation object \mathcal{E}_v that is (i) compact and (ii) faithful to f . In homogeneous graphs, model-agnostic explainers such as GNNExplainer seek a small subgraph and a subset of node features that maximize fidelity to the prediction. In our setting, the explanation space is meta-path-factorized: explanations may be defined per view $G_v^{(m)}$ (e.g., edge masks or selected structures). When needed for semantic

interpretation, we summarize each $E_v^{(m)}$ into a nonnegative scalar *meta-path contribution score*, which we later compare against the model's semantic attention in our diagnostic (MP-AEA).

4 A Meta-Path-Consistent Explanation Protocol

Goal. Our objective is to enable a controlled empirical study of meta-path importance and the reliability of semantic-level meta-path attention. MetaXplain standardizes how existing post-hoc explainers are applied in the meta-path view domain to avoid invalid conclusions caused by heterogeneity.

4.1 MetaXplain: Consistency conditions for meta-path-aware post-hoc explanation

Context. As defined in Section 3, a meta-path-based HeteroGNN takes as input the local meta-path views $\mathcal{G}(v) = \{G_v^{(m)}\}_{m \in \mathcal{M}}$ and computes meta-path-specific embeddings $\{\mathbf{h}_v^{(m)}\}$ followed by a fusion $\mathbf{h}_v = \text{Fuse}(\{\mathbf{h}_v^{(m)}\})$ and prediction $f(v) = \text{Dec}(\mathbf{h}_v)$ (Equations (2)–(3)). Naively applying homogeneous explainers on a collapsed graph can yield confounded explanations due to: (i) *semantic collapse*, (ii) *relation confusion* under perturbation, and (iii) *fusion-induced suppression* in attribution. We therefore enforce three consistency conditions below.

4.1.1 C1: View-Factorized Explanation Domain.

Condition. Under MetaXplain, explanations are defined on the meta-path view set $\mathcal{G}(v) = \{G_v^{(m)}\}_{m \in \mathcal{M}}$ rather than a single collapsed graph. Equivalently, its output decomposes as

$$\mathcal{E}_v = \{E_v^{(m)}\}_{m \in \mathcal{M}}, \quad (4)$$

where each $E_v^{(m)}$ is supported on the corresponding view $G_v^{(m)}$. This condition prevents *semantic collapse* and ensures explanations remain interpretable at the semantic-channel level.

Applying a homogeneous explainer under C1. Let a standard explainer be Φ that outputs an explanation for a (homogeneous) local graph input: $E_v = \Phi(f, G_v, X)$. We define its meta-path lifting as

$$\Phi_{\text{MP}}(f, \mathcal{G}(v), X) := \{E_v^{(m)}\}_{m \in \mathcal{M}}, \quad (5)$$

i.e., the explainer now optimizes / searches over a factorized explanation space aligned with the meta-path views.

4.1.2 C2: Channel-Wise and Schema-Valid Perturbation.

Condition. A perturbation mechanism is *meta-path-consistent* if it is (i) *channel-wise* (independent across m) and (ii) *schema-valid* (restricted to view $G_v^{(m)}$ and type consistent). Formally, perturbations take the form $\{\delta^{(m)}\}_{m \in \mathcal{M}}$ where each $\delta^{(m)}$ acts only within $G_v^{(m)}$.

Math (disentangled masks and optional semantic gate). For mask-based explainers, we replace a single mask by per-view masks

$$M = \{M^{(m)}\}_{m \in \mathcal{M}}, \quad M^{(m)} \in [0, 1]^{|E(G_v^{(m)})|}, \quad (6)$$

and define a masked view $\widetilde{G}_v^{(m)} = G_v^{(m)} \odot M^{(m)}$ (masking only edges in $G_v^{(m)}$). This condition prevents *confounded perturbations* in which removing a shared structural element simultaneously disrupts multiple meta-path semantics.

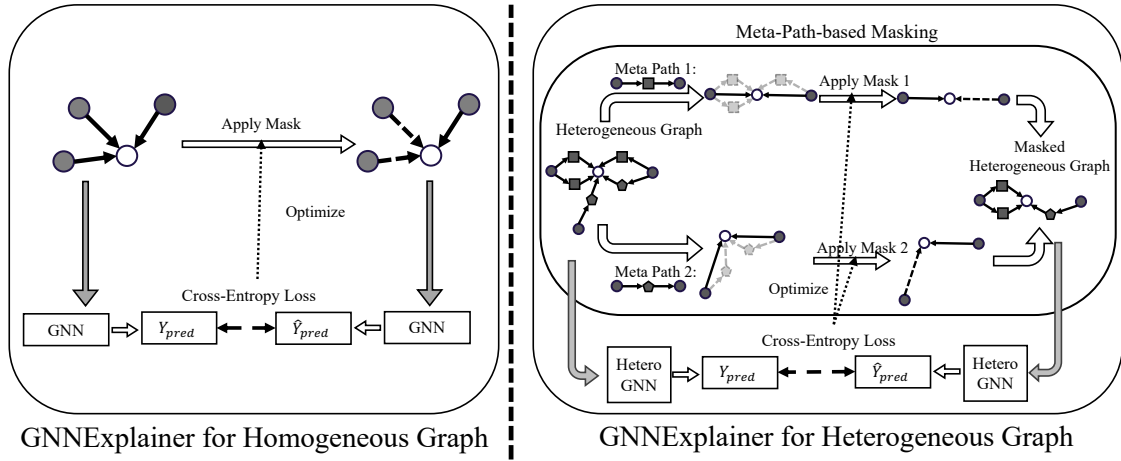


Figure 1: MetaXplain lifts GNNExplainer to the meta-path view domain.

Optionally, we introduce a meta-path gate $m_{\text{sem}} \in [0, 1]^{|\mathcal{M}|}$ and couple it to instance-level masks:

$$\tilde{M}^{(m)} := m_{\text{sem}}^{(m)} \cdot M^{(m)}, \quad \tilde{G}_v^{(m)} = G_v^{(m)} \odot \tilde{M}^{(m)}. \quad (7)$$

The explainer then optimizes its original objective (e.g., fidelity with sparsity regularization) over $\{\tilde{M}^{(m)}\}$.

4.1.3 C3: Fusion-Aware Attribution (Model-Agnostic).

Condition. An attribution is *fusion-aware* if it measures the contribution of each semantic channel *before* cross-channel fusion, and aggregates channel-wise contributions to explain $f(v)$.

Two practical options. Using the interface in Equations (2)–(3), define a channel contribution score $s_v^{(m)}$ and an aggregation $\text{Agg}(\cdot)$:

$$\text{Score}(v) = \text{Agg}(\{s_v^{(m)}\}_{m \in \mathcal{M}}). \quad (8)$$

This avoids *fusion-induced attribution artifacts*, where contributions can appear suppressed after $\text{Fuse}(\cdot)$ despite being locally important within a view.

(A) *Gradient-based (late-fusion gradients)*. Fusion-aware gradients can be computed either on the pre-fusion channel embeddings $\mathbf{h}_v^{(m)}$ or on the channel-specific inputs (e.g., features in view m), depending on the model accessibility:

$$s_{v,\text{GRAD}}^{(m)} \in \left\{ \left\| \nabla_{\mathbf{h}_v^{(m)}} \mathcal{L} \right\|, \left\| \nabla_{X^{(m)}} \mathcal{L} \right\| \right\}. \quad (9)$$

(B) *Gradient-free (fusion-aware occlusion / conditional fidelity)*. To remain post-hoc and model-agnostic, we estimate channel importance by occluding only channel m while holding all other channels fixed:

$$s_{v,\text{OCC}}^{(m)} = D\left(f\left(v; \{G_v^{(k)}\}_{k \in \mathcal{M}}\right), f\left(v; \{G_v^{(k)}\}_{k \neq m}, \emptyset^{(m)}\right)\right), \quad (10)$$

where $\emptyset^{(m)}$ is a schema-valid null view (e.g., $\tilde{M}^{(m)} = \mathbf{0}$) and $D(\cdot, \cdot)$ is a logit/probability divergence. Moreover, within-channel structure attribution follows by substituting $\emptyset^{(m)}$ with the masked view $\tilde{G}_v^{(m)}$ from C2 and measuring the conditional fidelity drop.

4.2 Explainers used in our empirical study

We evaluate representative post-hoc explainers spanning gradient-, perturbation-, and Shapley-style families. Under MetaXplain, each explainer is applied in the meta-path view domain and constrained by C1–C3. We emphasize that these are representative choices for our empirical study; the protocol is compatible with other post-hoc explainers.

Local view extraction and notation. Given a target node v , we extract a k -hop ego neighborhood within each meta-path view $G^{(m)}$ and re-index to a compact local graph $G_v^{(m)}$ for efficient explanation. This yields a list of sparse local adjacencies $\{A^{(m)}\}_{m=1}^M$ (one per meta-path) and a local feature matrix X shared across views. When an explainer requires feature perturbations conditioned on a specific view, we use per-view feature copies $\{X^{(m)}\}$ while keeping the adjacency list fixed.

Gradient heatmap (Grad). Under C1, Grad produces a view-indexed node-importance mask per meta-path view. For a target node v and its predicted class c^* , we compute gradients of the node-level loss with respect to node features and take the ℓ_2 norm across feature dimensions as a node score. Concretely, for node i in view m ,

$$I_{\text{Grad}}^{(m)}(i) = \left\| \frac{\partial \mathcal{L}(v, c^*)}{\partial x_i^{(m)}} \right\|_2. \quad (11)$$

To realize meta-path-conditioned gradients, when the predictor supports multi-feature inputs, we pass a list of feature tensors (one per meta-path) with independent gradient tracking, while keeping the meta-path adjacency list $\{A^{(m)}\}$ fixed. The resulting explanation is the set of node masks $\{I_{\text{Grad}}^{(m)}\}_{m=1}^M$, one per view.

GNNExplainer. Under C1–C2, we apply GNNExplainer with channel-wise edge masks restricted to each view and return the per-view mask set $\{M_A^{(m)}\}$. Given view m with local adjacency $A^{(m)}$, we optimize a continuous edge mask $M_A^{(m)} \in \mathbb{R}^{|\mathcal{E}^{(m)}|}$ (activated by sigmoid or ReLU), and (optionally) a feature mask $M_X \in \mathbb{R}^d$ shared across views. The masked input is formed by reweighting edges

within each view and masking features:

$$\tilde{A}^{(m)} = A^{(m)} \odot g(M_A^{(m)}), \quad \tilde{X} = X \odot h(M_X), \quad (12)$$

where $g(\cdot)$ is the configured edge-mask activation and $h(\cdot)$ is either identity or sigmoid. We then minimize a prediction-preservation loss with sparsity and entropy regularization (and an optional Laplacian term):

$$\begin{aligned} \min_{\{M_A^{(m)}\}, M_X} & \mathcal{L}_{\text{pred}}\left(f(\{\tilde{A}^{(m)}\}, \tilde{X}); v\right) + \lambda_{\text{size}} \sum_m \|g(M_A^{(m)})\|_1 \\ & + \lambda_{\text{ent}} \sum_m \mathcal{H}(g(M_A^{(m)})) + \lambda_{\text{lap}} \mathcal{L}_{\text{lap}}. \end{aligned} \quad (13)$$

When feature masking is enabled, we add analogous size/entropy terms for $h(M_X)$. All meta-path masks are optimized jointly but remain view-specific in output, yielding $\{g(M_A^{(m)})\}_{m=1}^M$ as meta-path-aware edge explanations.

In the main paper we focus on Grad and GNNExplainer as representative explainers; additional perturbation- and Shapley-style instantiations (and full results) are reported in the Appendix.

4.3 Metric: Meta-Path Attention-Explanation Alignment (MP-AEA)

Motivated by evidence that attention weights need not faithfully reflect feature importance [9, 16], we propose **MP-AEA** as a diagnostic that tests whether semantic meta-path attention *aligns with or decouples from* explanation-derived meta-path contributions across random runs.

4.3.1 Meta-path contribution scores from view-factorized explanations. Given a target node v , a MetaXplain instantiation outputs a view-factorized explanation object $\mathcal{E}_v = \{E_v^{(m)}\}_{m \in \mathcal{M}}$ (C1), where each $E_v^{(m)}$ is supported on view $G_v^{(m)}$. To compare against semantic attention, we summarize each view-level explanation into a non-negative scalar meta-path contribution score $s_v^{(m)} \in \mathbb{R}_{\geq 0}$: $s_v^{(m)} = \text{Agg}(E_v^{(m)})$, where $\text{Agg}(\cdot)$ is an aggregation operator consistent with the explainer output type. For node-attribution explainers (e.g., Grad, PGM-Explainer), we use $\text{Agg}(E_v^{(m)}) = \sum_{u \in V(G_v^{(m)})} I_v^{(m)}(u)$; for edge-attribution explainers (e.g., GNNExplainer, GNNShap), we use $\text{Agg}(E_v^{(m)}) = \sum_{e \in \mathcal{E}(G_v^{(m)})} w_v^{(m)}(e)$.

Optionally, to explicitly satisfy fusion-aware attribution (C3(B)), $s_v^{(m)}$ can be defined via channel occlusion:

$$s_v^{(m)} = D\left(f(v; \mathcal{G}(v)), f\left(v; \mathcal{G}(v) \setminus G_v^{(m)}, \emptyset^{(m)}\right)\right), \quad (14)$$

where $\emptyset^{(m)}$ is a schema-valid null view (e.g., all-zero mask on $G_v^{(m)}$) and $D(\cdot, \cdot)$ is a logit/probability divergence. Unless stated otherwise, we use Grad-based $E_v^{(m)}$ in our experiments.

4.3.2 Global explanation-derived meta-path vector. Let \mathcal{T} denote the test node set. We first normalize per-node contributions across meta-paths $\tilde{s}_v^{(m)} = \frac{s_v^{(m)}}{\sum_{m' \in \mathcal{M}} s_v^{(m')}}$. We then aggregate to a dataset-level vector $\mathbf{S} \in \mathbb{R}^{|\mathcal{M}|}$:

$$\mathbf{S}_m = \frac{1}{|\mathcal{T}|} \sum_{v \in \mathcal{T}} \tilde{s}_v^{(m)}. \quad (15)$$

\mathbf{S}_m estimates the overall contribution of meta-path m according to the chosen post-hoc explainer.

4.3.3 Alignment with semantic attention across runs. Let $\mathbf{A} \in \mathbb{R}^{|\mathcal{M}|}$ be the model’s semantic attention distribution over meta-path channels (after softmax normalization; e.g., HAN’s semantic-level attention). We train the model with R random seeds, obtaining vector pairs $\{(\mathbf{A}^{(r)}, \mathbf{S}^{(r)})\}_{r=1}^R$. For each meta-path m , MP-AEA computes rank correlation between attention and explanation across runs:

$$\text{MP-AEA}_\tau(m) = \tau([\mathbf{A}_m^{(1)}, \dots, \mathbf{A}_m^{(R)}], [\mathbf{S}_m^{(1)}, \dots, \mathbf{S}_m^{(R)}]), \quad (16)$$

$$\text{MP-AEA}_\rho(m) = \rho([\mathbf{A}_m^{(1)}, \dots, \mathbf{A}_m^{(R)}], [\mathbf{S}_m^{(1)}, \dots, \mathbf{S}_m^{(R)}]). \quad (17)$$

Interpretation. High MP-AEA indicates that semantic attention consistently tracks explanation-derived meta-path contributions across runs, while low or insignificant MP-AEA reveals an interpretability gap where attention is decoupled from post-hoc importance. MP-AEA measures consistency, not necessarily correctness.

Binary meta-paths. When $|\mathcal{M}| = 2$, both \mathbf{A} and \mathbf{S} are complementary (summing to 1), so correlation magnitudes are identical for both meta-paths. We therefore report a single MP-AEA score per model–dataset pair.

5 Experiments

We design experiments as a diagnostic empirical study of meta-path importance and the reliability of semantic-level meta-path attention.

We organize the study around four research questions:

- RQ1:** How faithful are post-hoc explainers under MetaXplain after being lifted to the meta-path view set?
- RQ2:** How much do different meta-path channels contribute to predictive performance under controlled interventions?
- RQ3:** Does semantic-level attention reliably reflect meta-path importance?
- RQ4:** Can explanations recover task-relevant substructures that are sufficient for prediction?

5.1 Experiment Setup

5.1.1 Evaluation Metrics. We evaluate explanation quality using the standard faithfulness metrics *Fidelity*_− and *Fidelity*₊ [2], which quantify sufficiency and necessity under controlled masking, respectively. For readability, we report $1 - \text{Fidelity}_-$ instead of *Fidelity*_−. To complement local faithfulness with downstream utility, we also report Macro-F1 and Micro-F1 on the prediction task under the masked inputs. To standardize comparisons across explainers with different output formats (edge masks, node masks, and edge+feature masks), we evaluate explanations using hard top- k masking at a fixed sparsity level. Unless otherwise stated, we set sparsity to 0.25 for each mask type.

5.1.2 Benchmarks. We conduct experiments on three benchmark heterogeneous graphs: ACM, DBLP, and IMDB, following the pre-processing and splits in [29] for reproducibility. These three datasets all contain two meta-paths.

5.1.3 Models. We evaluate two meta-path-based predictors: HAN [23] and HAN-GCN, a HAN variant that replaces GAT layers with GCN layers. On top of each trained predictor, we apply MetaXplain with

Table 1: Results of explanation models on HAN/HAN-GCN predictor for three datasets. Higher is better for all metrics.

Predictor	HeteroGNN	Model	Mask Type	1 - <i>Fidelity</i> _−	<i>Fidelity</i> ₊	Macro - <i>F1</i>	Micro - <i>F1</i>
HAN	GNNEExplainer	edge+feature	88.20 ± 2.32	2.60 ± 0.80	84.02 ± 2.17	83.60 ± 2.33	
		edge+feature	85.80 ± 2.56	3.00 ± 0.63	80.63 ± 2.21	80.00 ± 2.19	
	xPath	edge	81.60 ± 3.44	2.80 ± 0.75	79.77 ± 2.94	78.80 ± 3.31	
	GraphSVX	edge	94.60 ± 2.15	9.20 ± 1.47	87.95 ± 1.15	87.60 ± 1.20	
	GNNShap	edge	94.80 ± 1.33	10.40 ± 1.36	87.34 ± 1.12	87.00 ± 1.10	
	RandomEdgeMask	edge	87.60 ± 2.65	2.20 ± 1.47	82.47 ± 3.33	81.80 ± 3.43	
ACM	Grad	node	97.60 ± 0.80	32.20 ± 3.92	91.49 ± 0.84	91.40 ± 0.80	
	PGM-Explainer	node	95.40 ± 1.85	15.60 ± 5.95	90.08 ± 1.15	90.00 ± 1.10	
	RandomNodeMask	node	89.20 ± 2.40	3.80 ± 1.72	85.87 ± 2.02	85.40 ± 2.15	
	GNNEExplainer	edge+feature	60.60 ± 8.16	16.80 ± 3.82	59.75 ± 7.08	60.40 ± 7.00	
	RandomEdgeAndFeatureMask	edge+feature	72.40 ± 7.20	21.80 ± 5.42	69.98 ± 8.64	71.80 ± 6.62	
	xPath	edge	75.60 ± 3.72	19.80 ± 8.47	77.62 ± 5.97	77.20 ± 6.01	
HAN-GCN	GraphSVX	edge	77.40 ± 7.00	21.80 ± 4.31	76.40 ± 7.20	76.80 ± 6.43	
	GNNShap	edge	80.80 ± 11.37	24.40 ± 2.24	77.39 ± 10.60	78.40 ± 8.66	
	RandomEdgeMask	edge	73.80 ± 7.11	20.40 ± 6.44	72.16 ± 7.24	73.20 ± 5.98	
	Grad	node	93.00 ± 5.02	32.40 ± 3.56	88.21 ± 5.10	88.00 ± 5.10	
	PGM-Explainer	node	84.40 ± 4.08	28.60 ± 5.24	82.85 ± 3.43	82.60 ± 3.26	
	RandomNodeMask	node	75.20 ± 7.00	21.40 ± 6.89	73.55 ± 7.78	74.60 ± 6.59	
DBLP	GNNEExplainer	edge+feature	95.60 ± 2.06	1.60 ± 1.50	92.39 ± 2.06	94.80 ± 1.47	
	RandomEdgeAndFeatureMask	edge+feature	78.40 ± 9.35	1.60 ± 0.80	66.86 ± 8.44	77.60 ± 10.29	
	xPath	edge	93.00 ± 1.90	2.80 ± 1.17	94.52 ± 1.41	95.00 ± 1.10	
	GraphSVX	edge	97.00 ± 0.63	1.80 ± 1.47	92.75 ± 0.71	95.00 ± 0.63	
	GNNShap	edge	99.40 ± 0.49	7.40 ± 1.85	91.70 ± 0.65	94.80 ± 0.40	
	RandomEdgeMask	edge	96.00 ± 1.10	1.00 ± 1.10	92.78 ± 1.66	95.20 ± 1.17	
HAN	Grad	node	94.40 ± 3.26	8.80 ± 3.49	90.56 ± 2.11	92.40 ± 2.42	
	PGM-Explainer	node	95.00 ± 0.63	4.20 ± 0.75	91.78 ± 0.70	94.20 ± 0.40	
	RandomNodeMask	node	82.00 ± 8.56	2.00 ± 0.63	74.11 ± 7.58	81.60 ± 8.80	
	GNNEExplainer	edge+feature	71.60 ± 1.02	5.80 ± 0.75	62.00 ± 1.82	68.60 ± 1.50	
	RandomEdgeAndFeatureMask	edge+feature	93.20 ± 1.33	6.40 ± 0.49	87.63 ± 2.20	91.40 ± 1.62	
	xPath	edge	81.20 ± 2.79	5.40 ± 1.20	73.61 ± 2.61	78.60 ± 2.15	
HAN-GCN	GraphSVX	edge	90.60 ± 1.85	6.80 ± 0.75	84.37 ± 1.52	87.20 ± 1.17	
	GNNShap	edge	94.40 ± 0.80	11.60 ± 1.50	88.11 ± 2.95	91.40 ± 2.24	
	RandomEdgeMask	edge	93.80 ± 0.40	6.60 ± 1.02	87.76 ± 2.46	91.20 ± 1.72	
	Grad	node	93.60 ± 0.49	7.20 ± 0.75	84.88 ± 0.14	89.00 ± 0.00	
	PGM-Explainer	node	94.00 ± 1.41	6.80 ± 0.75	88.99 ± 2.77	92.20 ± 1.94	
	RandomNodeMask	node	93.60 ± 0.49	6.40 ± 0.80	87.74 ± 1.36	91.40 ± 1.02	
HAN	GNNEExplainer	edge+feature	68.80 ± 2.14	7.20 ± 1.72	48.22 ± 4.04	51.20 ± 2.79	
	RandomEdgeAndFeatureMask	edge+feature	56.80 ± 4.87	14.20 ± 1.72	40.61 ± 3.15	47.60 ± 3.20	
	xPath	edge	63.60 ± 2.06	8.80 ± 2.14	45.93 ± 1.95	47.60 ± 1.85	
	GraphSVX	edge	93.40 ± 2.50	35.80 ± 1.94	54.91 ± 1.69	55.80 ± 1.72	
	GNNShap	edge	89.20 ± 1.94	44.40 ± 1.02	52.87 ± 1.28	54.80 ± 1.60	
	RandomEdgeMask	edge	66.20 ± 4.71	8.40 ± 1.62	48.27 ± 2.56	50.60 ± 2.33	
IMDB	Grad	node	82.00 ± 2.19	35.20 ± 4.92	49.42 ± 1.71	49.60 ± 2.06	
	PGM-Explainer	node	79.40 ± 3.50	27.60 ± 2.06	48.70 ± 2.10	49.00 ± 2.00	
	RandomNodeMask	node	63.40 ± 3.77	11.00 ± 1.26	44.43 ± 4.23	49.40 ± 3.20	
	GNNEExplainer	edge+feature	65.20 ± 2.04	5.20 ± 1.33	42.89 ± 3.26	48.00 ± 2.68	
	RandomEdgeAndFeatureMask	edge+feature	60.80 ± 3.54	14.00 ± 3.29	36.35 ± 3.72	45.20 ± 2.32	
	xPath	edge	60.00 ± 5.55	3.80 ± 1.17	43.29 ± 2.78	48.80 ± 1.17	
HAN-GCN	GraphSVX	edge	77.40 ± 3.38	13.60 ± 1.96	45.22 ± 1.07	50.20 ± 1.17	
	GNNShap	edge	78.40 ± 2.42	23.40 ± 3.88	47.30 ± 1.68	51.40 ± 2.06	
	RandomEdgeMask	edge	67.20 ± 0.40	6.20 ± 2.32	42.24 ± 1.86	48.40 ± 1.50	
	Grad	node	89.80 ± 1.33	33.20 ± 1.47	50.43 ± 4.82	52.60 ± 4.88	
	PGM-Explainer	node	87.20 ± 2.14	26.00 ± 3.41	50.81 ± 3.16	51.20 ± 2.71	
	RandomNodeMask	node	68.40 ± 1.20	9.80 ± 2.23	43.80 ± 4.38	49.20 ± 3.87	

five representative explainers: Grad [18, 21], GNNEExplainer [27], PGM-Explainer [22], GraphSVX [4], and GNNShap [1]. We compare against the heterogeneous baseline xPath [11], and type-matched random baselines (edge masking, node masking, and edge+feature masking).

5.2 Effectiveness

We first address RQ1 by characterizing how representative post-hoc explainers behave when applied under the MetaXplain protocol (C1–C3), which standardizes the explanation domain (meta-path

views), perturbation semantics, and evaluation budget. We provide a controlled comparison across explanation families and identify robust patterns and failure modes that matter for subsequent attention-importance diagnostics.

Table 1 report faithfulness and downstream performance on ACM, DBLP, and IMDB for both HAN and HAN-GCN over 5 random seeds. To isolate explanation quality from mask budget, we compare methods within each **mask type** (edge+feature, edge, node) against a type-matched random baseline at the same sparsity.

Overall effectiveness (RQ1). Across datasets and backbones, most MetaXplain-applied explainers improve over their corresponding

random controls, indicating that view-factorized explanations recover non-trivial, prediction-relevant evidence. However, the magnitude and stability of these improvements are strongly *backbone-dependent* and vary across explainer families.

Edge+feature masking: *GNNEExplainer* is *backbone-sensitive*. *GNNEExplainer* performs strongly on HAN (e.g., consistent improvements over *RandomEdgeAndFeatureMask* across datasets), but can degrade sharply on HAN-GCN. We attribute this to a soft-mask vs. hard-mask gap: *GNNEExplainer* optimizes continuous reweighting, but evaluation uses hard top- k sparsification. This discretization-induced shift is amplified under GCN-style aggregation and normalization, making HAN-GCN explanations brittle compared to HAN.

Edge masking: *Shapley-style explainers* are *comparatively robust*. xPath can be competitive in some settings, but its behavior is not consistently superior to type-matched random controls across datasets/backbones. In contrast, Shapley-style explainers (GraphSVX and GNNShap) tend to be more robust: they frequently exceed both xPath and *RandomEdgeMask*, and show smaller sensitivity to the choice of backbone. Moreover, GNNShap often improves over GraphSVX, consistent with edge-level Shapley attribution being better aligned with edge-masking evaluation than surrogate node-centric approximations [1].

Node masking: *Grad* is *consistently strong*. Within node-masking methods, *Grad* is typically the strongest and substantially exceeds *RandomNodeMask*. PGM-Explainer also improves over the random control, but is generally less competitive than *Grad*. This gap suggests headroom for methods that more directly model meta-path-specific evidence under heterogeneous semantics, motivating our later focus on meta-path contribution estimation and attention alignment (RQ2–RQ3).

Backbone sensitivity: HAN vs. HAN-GCN. Finally, we observe higher variance and stronger method sensitivity on HAN-GCN than on HAN (e.g., larger standard deviations for several edge explainers on ACM/HAN-GCN). This indicates that the underlying within-view aggregation and cross-view fusion mechanisms play a central role in explanation stability, and motivates our subsequent diagnostic analysis of semantic attention and meta-path importance (RQ3).

Table 2: MP-AEA scores across 100 random seeds.

Metric	ACM	DBLP	IMDB
HAN			
Kendall's tau (P-value)	0.439 (1e-10)	0.053 (0.432)	0.700 (6e-25)
Spearman (P-value)	0.618 (8e-12)	0.069 (0.496)	0.872 (4e-32)
HAN-GCN			
Kendall's tau (P-value)	0.414 (1e-9)	0.601 (8e-19)	0.860 (8e-37)
Spearman (P-value)	0.562 (1e-9)	0.793 (8e-23)	0.961 (1e-56)

5.3 Attention can decouple from meta-path importance (RQ2–RQ3)

This section addresses the central diagnostic question of our study: **when does semantic-level meta-path attention reflect meta-path importance, and when can it decouple?** We probe meta-path importance using explanation-derived per-view contribution scores (Section 4.3) and quantify attention reliability using **MP-AEA**, which measures rank correlation between learned semantic attention and explanation-derived meta-path contributions across random runs. In addition, we perform *controlled attention interventions* (forcing attention to a single meta-path or to a uniform mixture) to test the empirical utility of each meta-path channel.

Why HAN-GCN is a cleaner probe of meta-path importance. HAN couples edge-level attention within each meta-path view (GAT) with semantic-level attention across meta-path channels, so strong performance may come from neighbor selection within a view even when a channel is down-weighted. Prior works [12, 15] show that well-tuned attention-based GNNs (e.g., GAT) can be highly competitive on heterogeneous benchmarks, suggesting edge attention can partially substitute for explicit heterogeneous semantics. We therefore also evaluate HAN-GCN, which removes within-view edge attention and makes semantic attention the primary mechanism for weighting meta-path channels. This separation helps interpret whether attention behaves as a proxy for channel importance rather than as one component among multiple attention mechanisms.

5.3.1 Does Attention Align with Importance? (RQ3). We quantify the agreement between semantic attention and explanation-derived meta-path contributions using MP-AEA (Section 4.3). Tables 2 report Kendall's τ and Spearman's ρ correlations between (i) semantic attention weights and (ii) *Grad*-based meta-path contribution scores across 100 random seeds.

Key observation: both alignment and decoupling regimes exist. On IMDB, both HAN and HAN-GCN exhibit consistently high correlations, indicating that semantic attention is a stable proxy for explanation-derived meta-path importance in this setting. In contrast, on DBLP the correlation for HAN is statistically insignificant, revealing a clear *decoupling* regime where attention does not reliably track meta-path contribution estimates. Notably, alignment is generally stronger under HAN-GCN than HAN across datasets, consistent with HAN-GCN isolating semantic attention from within-view edge attention.

5.3.2 Empirical Utility of Meta-Paths (RQ2). We next test whether meta-paths carry materially different predictive signal via controlled semantic attention interventions (Figures 2 and 5 in Appendix). Specifically, we compare the learned attention (*Original*) with three controlled configurations: forcing attention to a single meta-path (*Meta-Path 1* or *Meta-Path 2*) and a uniform mixture (*Balanced*).

Meta-path utility is dataset-dependent and can expose attention failure modes. On ACM and DBLP, performance is strongly sensitive to path selection: forcing attention to the empirically stronger meta-path nearly matches the learned model, while forcing the weaker meta-path substantially degrades performance. This indicates that the two semantic channels contain materially different task-relevant signal. On IMDB, we observe a distinct behavior: under HAN-GCN,

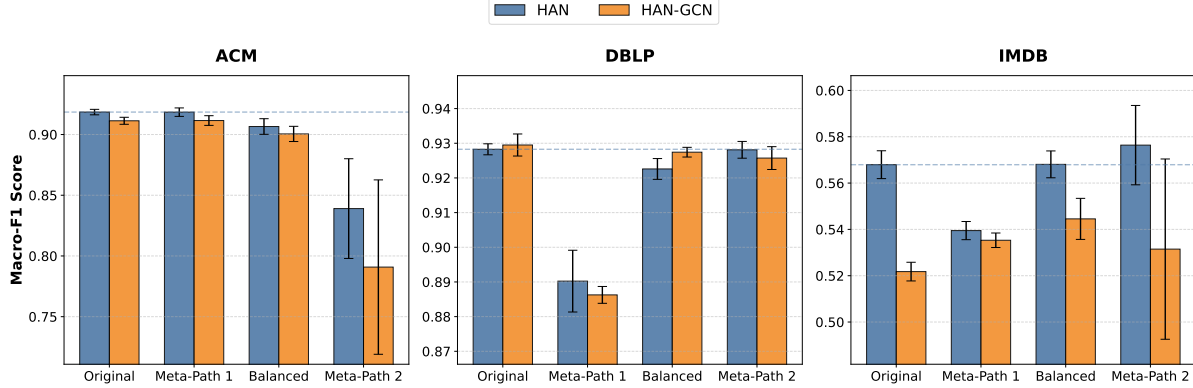


Figure 2: Macro-F1 under controlled semantic attention interventions. Error bars show std. over 5 runs.

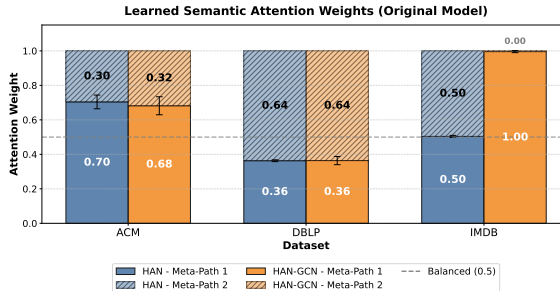


Figure 3: Learned semantic attention weights. Error bars indicate std.

semantic attention collapses toward a single meta-path, yet the *Balanced* configuration performs better. This suggests that attention can over-commit to one channel and miss complementary evidence, even when both meta-paths are useful under controlled mixing.

Connection to subgraph recoverability. Importantly, a decoupling or over-commitment regime does not imply that meta-path signal is absent. As shown in Section 5.4, retraining on explanation-induced subgraphs can substantially improve IMDB performance for HAN-GCN, consistent with an explanation-as-denoising effect in noisy regimes. Together, these results support our main message: *semantic attention is not universally reliable as a proxy for meta-path importance*, and its reliability depends on the dataset and backbone.

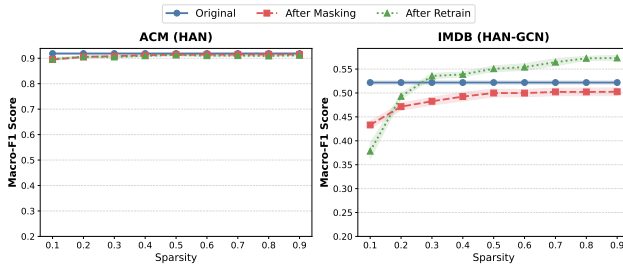


Figure 4: Recoverability from explanation-induced subgraphs. Shaded regions show std. over 5 runs.

5.4 Recoverability from explanation-induced subgraphs (RQ4)

To address RQ4, we use explanation-induced subgraph extraction as a *diagnostic intervention*: if a post-hoc explanation identifies task-relevant evidence, then the subgraph induced by top-ranked nodes should retain substantial predictive signal. Importantly, this test separates two notions: (i) *inference-time sufficiency* under hard pruning (which can introduce distribution shift), and (ii) *recoverability* of the signal after retraining on the extracted structure.

Protocol. For each target node v , we construct an explanation-induced subgraph by retaining the top-ranked nodes under Grad at a prescribed sparsity level (fraction removed). We then compare three settings: *Original* (performance on the full graph), *After Masking* (inference on the extracted subgraph without retraining), and *After Retrain* (training a new model on the extracted subgraph with the same hyperparameters). Figure 4 reports Macro-F1 under varying sparsity.

Case (i): ACM with HAN – concentrated evidence and mild distribution shift. On ACM/HAN, *After Retrain* remains close to *Original* even at high sparsity, indicating that the task-relevant evidence is concentrated in a small neighborhood that the explainer consistently recovers. Moreover, the relatively small gap between *After Masking* and *Original* suggests that the extracted subgraphs remain largely in-distribution for the trained attention-based backbone, so pruning does not severely disrupt inference.

Case (ii): IMDB with HAN-GCN – recoverability and an explanation-as-denoising regime. On IMDB/HAN-GCN, hard pruning causes a clear drop in *After Masking*, reflecting sensitivity of GCN-style aggregation to structural removal and potential distribution shift. However, *After Retrain* substantially recovers this drop and can even exceed *Original* at moderate-to-high sparsity. This behavior is consistent with an *explanation-as-denoising* regime: pruning weakly relevant neighborhoods can act as a beneficial inductive bias for retraining by reducing noise in the computation graph.

Takeaway. These results support a key theme of our study: even when semantic attention can decouple from meta-path importance (RQ3), post-hoc explanations can still identify substructures that retain recoverable predictive signal. The gap between *After Masking* and *After Retrain* further highlights that evaluating explanations

solely by inference-time masking can conflate explanation quality with distribution shift, especially for GCN-style backbones.

6 Conclusion

We conducted an empirical study of a common interpretability assumption in meta-path-based heterogeneous GNNs: whether semantic-level meta-path attention can be treated as a proxy for meta-path importance. To make this question testable without changing the predictor, we introduced **MetaXplain**, a meta-path-consistent post-hoc explanation protocol that lifts existing explainers into the meta-path view domain via view-factorized explanations, schema-valid channel-wise perturbations, and fusion-aware attribution, and we proposed **MP-AEA** to quantify attention-importance agreement across random runs. Experiments on ACM, DBLP, and IMDB with HAN and HAN-GCN show that lifted explainers generally outperform type-matched random baselines but are backbone-sensitive, while MP-AEA reveals both alignment and decoupling regimes where attention can or cannot reliably track explanation-derived meta-path contributions depending on the dataset/backbone. Finally, explanation-induced subgraphs often retain recoverable predictive signal after retraining and can even improve performance in noisy regimes, suggesting an explanation-as-denoising effect and highlighting that masking-only evaluation can conflate explanation quality with distribution shift.

References

- [1] Selahattin Akkas and Ariful Azad. 2024. Gnnshap: Scalable and accurate gnn explanation using shapley values. In *Proceedings of the ACM Web Conference 2024*. 827–838.
- [2] Kenza Amara, Rex Ying, Zitao Zhang, Zhihao Han, Yinan Shan, Ulrik Brandes, Sebastian Schemm, and Ce Zhang. 2022. GraphFramEx: Towards Systematic Evaluation of Explainability Methods for Graph Neural Networks. In *LOG IN*.
- [3] Federico Baldassarre and Hossein Azizpour. 2019. Explainability Techniques for Graph Convolutional Networks. *ArXiv* abs/1905.13686 (2019).
- [4] Alexandre Duval and Fragkiskos D Malliaros. 2021. Graphsvx: Shapley value explanations for graph neural networks. In *Joint European conference on machine learning and knowledge discovery in databases*. Springer, 302–318.
- [5] Wensi Fan, Yao Ma, Qing Li, Yuan He, Yihong Eric Zhao, Jiliang Tang, and Dawei Yin. 2019. Graph Neural Networks for Social Recommendation. *The World Wide Web Conference* (2019).
- [6] Chen Feng, Yumam He, Shiyang Wen, Guojun Liu, Liang Wang, Jian Xu, and Bo Zheng. 2022. DC-GNN: Decoupled Graph Neural Networks for Improving and Accelerating Large-Scale E-commerce Retrieval. *Companion Proceedings of the Web Conference 2022* (2022).
- [7] Xinyu Fu, Jian Zhang, Ziqiao Meng, and Irwin King. 2020. Magnn: Metapath aggregated graph neural network for heterogeneous graph embedding. In *Proceedings of The Web Conference 2020*. 2331–2341.
- [8] Peter J. Gawthrop and Michael Pan. 2022. Network Thermodynamics of Biological Systems: A Bond Graph Approach. *bioRxiv* (2022).
- [9] Sarthak Jain and Byron C. Wallace. 2019. Attention is not Explanation. In *North American Chapter of the Association for Computational Linguistics*.
- [10] Dominik Köhler and Stefan Heindorf. 2024. Utilizing Description Logics for Global Explanations of Heterogeneous Graph Neural Networks. *ArXiv* abs/2405.12654 (2024).
- [11] Tong Li, Jiale Deng, Yanyan Shen, Luyu Qiu, Huang Yongxiang, and Caleb Chen Cao. 2023. Towards Fine-Grained Explainability for Heterogeneous Graph Neural Network. *Proceedings of the AAAI Conference on Artificial Intelligence* 37, 7 (Jun. 2023), 8640–8647. doi:10.1609/aaai.v37i7.26040
- [12] Zhaoqing Li, Maiqi Jiang, Shengyuan Chen, Bo Li, Guorong Chen, and Xiao Huang. 2025. Automated Heterogeneous Network learning with Non-Recursive Message Passing. *arXiv preprint arXiv:2501.07598* (2025).
- [13] Dongsheng Luo, Wei Cheng, Dongkuan Xu, Wenchao Yu, Bo Zong, Haifeng Chen, and Xiang Zhang. 2020. Parameterized Explainer for Graph Neural Network. *Advances in Neural Information Processing Systems* 33 (2020).
- [14] Gengsi Lv, C. Zhang, and Lei Chen. 2023. HENCE-X: Toward Heterogeneity-agnostic Multi-level Explainability for Deep Graph Networks. *Proc. VLDB Endow.* 16 (2023), 2990–3003.
- [15] Qingsong Lv, Ming Ding, Qiang Liu, Yuxiang Chen, Wenzheng Feng, Siming He, Chang Zhou, Jianguo Jiang, Yuxiao Dong, and Jie Tang. 2021. Are we really making much progress? revisiting, benchmarking and refining heterogeneous graph neural networks. In *Proceedings of the 27th ACM SIGKDD conference on knowledge discovery & data mining*. 1150–1160.
- [16] Akash Kumar Mohankumar, Preksha Nema, Sharan Narasimhan, Mitesh M. Khapra, Balaji Vasan Srinivasan, and Balaraman Ravindran. 2020. Towards Transparent and Explainable Attention Models. In *Annual Meeting of the Association for Computational Linguistics*.
- [17] Seth A Myers, Aneesh Sharma, Pankaj Gupta, and Jimmy Lin. 2014. Information network or social network? The structure of the Twitter follow graph. In *Proceedings of the 23rd international conference on world wide web*. 493–498.
- [18] Phillip E. Pope, Soheil Kolouri, Mohammad Rostami, Charles E. Martin, and Heiko Hoffmann. 2019. Explainability Methods for Graph Convolutional Neural Networks. In *2019 IEEE/CVF Conference on Computer Vision and Pattern Recognition (CVPR)*. 10764–10773. doi:10.1109/CVPR.2019.01103
- [19] Ramprasaath R. Selvaraju, Michael Cogswell, Abhishek Das, Ramakrishna Vedantam, Devi Parikh, and Dhruv Batra. 2017. Grad-CAM: Visual explanations from deep networks via gradient-based localization. In *Proceedings of the IEEE international conference on computer vision*. 618–626.
- [20] Yong-Min Shin, Siqiang Li, Xin Cao, and Won-Yong Shin. 2024. Revisiting Attention Weights as Interpretations of Message-Passing Neural Networks. *ArXiv* abs/2406.04612 (2024).
- [21] Karen Simonyan. 2013. Deep inside convolutional networks: Visualising image classification models and saliency maps. *arXiv preprint arXiv:1312.6034* (2013).
- [22] Minh Vu and My T Thai. 2020. Pgm-explainer: Probabilistic graphical model explanations for graph neural networks. *Advances in neural information processing systems* 33 (2020), 12225–12235.
- [23] Xiao Wang, Houye Ji, Chuan Shi, Bai Wang, Yanfang Ye, Peng Cui, and Philip S Yu. 2019. Heterogeneous graph attention network. In *Proceedings of the 25th ACM SIGKDD international conference on knowledge discovery & data mining*. 1731–1739.
- [24] Sarah Wiegreffe and Yuval Pinter. 2019. Attention is not not Explanation. In *Conference on Empirical Methods in Natural Language Processing*.
- [25] Qiang Yang, Changsheng Ma, Qiannan Zhang, Xin Gao, Chuxu Zhang, and Xiangliang Zhang. 2023. Counterfactual Learning on Heterogeneous Graphs with Greedy Perturbation. *Proceedings of the 29th ACM SIGKDD Conference on Knowledge Discovery and Data Mining* (2023).
- [26] Xiaocheng Yang, Mingyu Yan, Shirui Pan, Xiaochun Ye, and Dongrui Fan. 2023. Simple and efficient heterogeneous graph neural network. In *Proceedings of the AAAI conference on artificial intelligence*, Vol. 37. 10816–10824.
- [27] Zhitao Ying, Dylan Bourgeois, Jiaxuan You, Marinka Zitnik, and Jure Leskovec. 2019. GNNExplainer: Generating explanations for graph neural networks. In *Advances in neural information processing systems*, Vol. 32.
- [28] Hao Yuan, Haiyang Yu, Jie Wang, Kang Li, and Shuiwang Ji. 2021. On Explainability of Graph Neural Networks via Subgraph Explorations. In *International Conference on Machine Learning*.
- [29] Seunghun Yun, Minbyul Jeong, Raehyun Kim, Hyunwoo J Kang, and Jinyoung Kim. 2019. Graph transformer networks. In *Advances in Neural Information Processing Systems*, Vol. 32.
- [30] Shichang Zhang, Jiani Zhang, Xiang Song, Soji Adeshina, Da Zheng, Christos Faloutsos, and Yizhou Sun. 2023. PaGE-Link: Path-based Graph Neural Network Explanation for Heterogeneous Link Prediction. *Proceedings of the ACM Web Conference 2023* (2023).

A Additional Results

A.1 Additional Analysis for Subgraph Fidelity

HAN: extracted subgraphs are largely sufficient on citation-style benchmarks. Across ACM and DBLP (Figure 6), *After Retrain* stays close to *Original* even at high sparsity, suggesting that predictive evidence is concentrated and that *GRAD* consistently recovers the most informative neighborhood. In these settings, *After Masking* also remains relatively stable, indicating that the pruned computation graph does not introduce severe distribution shift for an attention-based aggregator.

HAN-GCN: sensitivity to structural perturbations, but strong recoverability after retraining. For HAN-GCN on ACM (Figure 7), *After Masking* degrades more consistently with increasing sparsity compared to HAN, reflecting the greater sensitivity of a GCN-style

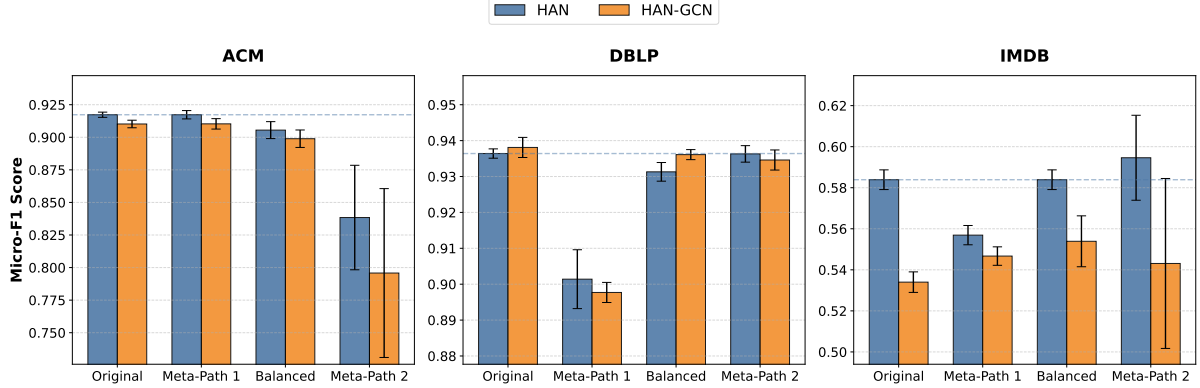


Figure 5: Micro-F1 under controlled semantic attention interventions. Error bars show std. over 5 runs.

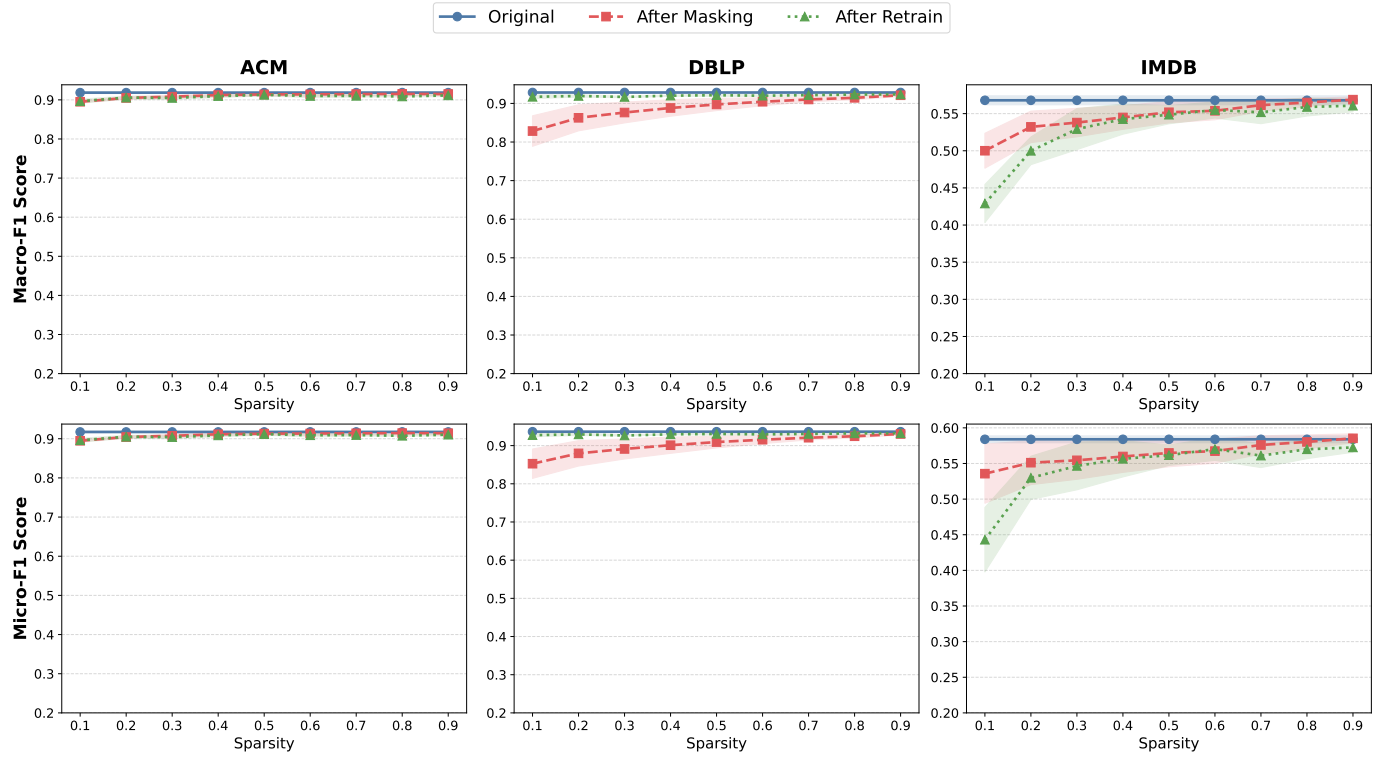


Figure 6: Recoverability from explanation-induced subgraphs. We evaluate the quality of explanation-identified subgraphs at varying sparsity levels (fraction of nodes removed). Three conditions are compared: *Original* (full graph performance), *After Masking* (inference on the extracted subgraph without retraining), and *After Retrain* (model retrained on the extracted subgraph). Shaded regions indicate std. over 5 runs.

aggregator to hard structural changes. However, *After Retrain* remains near *Original*, indicating that the pruned graphs still contain sufficient predictive signal and that the model can relearn effectively on the explanation-induced structure.

B Datasets

We evaluate MetaXplain on three widely used heterogeneous graph benchmarks for node classification: ACM, DBLP, and IMDB. These datasets differ in domain, node semantics, and relational structure, allowing us to assess explanation behavior across diverse heterogeneous settings. Dataset statistics are summarized in Table 3.

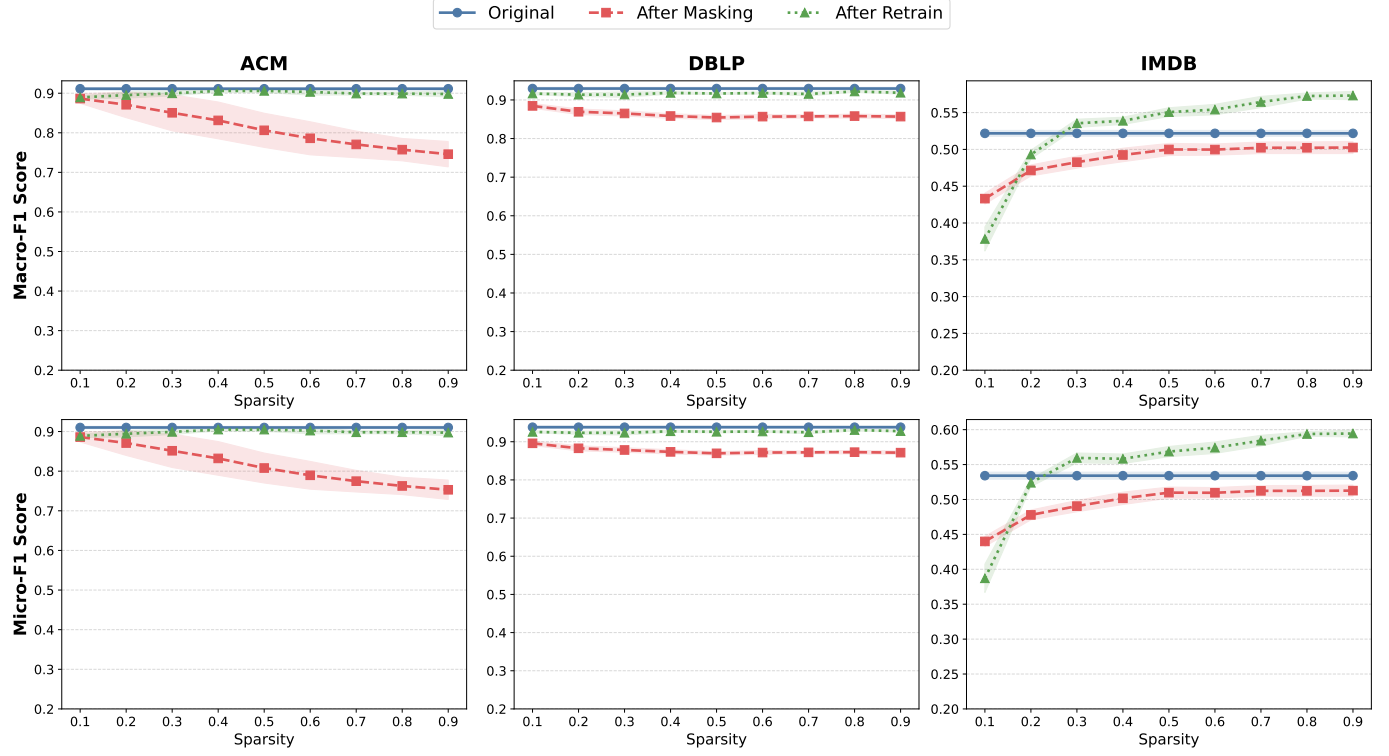


Figure 7: Recoverability from explanation-induced subgraphs. Shaded regions indicate std. over 5 runs.

ACM. ACM is a citation network with three node types: *papers* (P), *authors* (A), and *subjects* (S). Edges include paper–author (P – A), paper–subject (P – S), and paper–paper citations. The node classification task is to predict the research category of papers. Each paper is associated with a bag-of-words feature vector. Meta-paths such as P – A – P and P – S – P are used to model collaboration and topic-based semantics.

DBLP. DBLP is a bibliographic network consisting of three node types: *authors* (A), *papers* (P), and *conferences* (C). Edges encode relations such as author–paper (A – P), and paper–conference (P – C). The task is to classify *author* nodes into research areas. Node features are represented as bag-of-words vectors derived from paper titles. We construct 2 meta-path views (e.g., A – P – A , A – P – C – P – A) to capture distinct semantic relations between authors.

IMDB. IMDB is a movie network containing *movies* (M), *actors* (A), and *directors* (D). Edges represent acting and directing relationships. The task is multi-class movie genre classification. Node features are constructed from plot keywords. We define meta-paths such as M – A – M and M – D – M to encode shared cast and director information.

C Model Architectures and Training Hyperparameters

All heterogeneous GNN models are trained prior to explanation using fixed architecture and optimization settings, based on the original authors' reported hyperparameter settings. This section

Table 3: Statistics of heterogeneous graph datasets used for node classification.

Dataset	#Nodes	#Edges	# \mathcal{R}	#Feat.	Train	Val	Test
ACM	8,994	25,922	4	1,902	600	300	2,125
DBLP	18,405	67,946	4	334	800	400	2,857
IMDB	12,772	37,288	4	1,256	300	300	2,339

summarizes the shared training hyperparameters for HAN and HAN-GCN models used across all datasets.

Table 4: Training hyperparameters for heterogeneous GNN models.

Hyperparameter	HAN	HAN_GCN
Node-level aggregation	GAT	GCN
Hidden units	8	64
Attention heads	8	–
Dropout rate	0.6	0.6
Learning rate	0.01	0.01
Weight decay	0.001	0.001
Optimizer	Adam	Adam
Training epochs	200	200
Early stopping patience	100	100

Algorithm 2 GNNExplainer under MetaXplain

```

1: Input: Heterogeneous graph  $G$ , trained HeteroGNN  $f$ , meta-path set  $\mathcal{M}$ , target node  $v$ , hops  $k$ , optimization steps  $T$ 
2: Output: Meta-path-conditioned edge masks  $\{M_A^{(m)}\}_{m \in \mathcal{M}}$  and shared feature mask  $M_X$ 
3: Extract  $k$ -hop subgraph  $\mathcal{G}(v)$ 
4: Initialize edge mask  $M_A^{(m)}$  for each meta-path and shared feature mask  $M_X$ 
5: for  $t = 1$  to  $T$  do
6:   for  $m \in \mathcal{M}$  do
7:      $\tilde{A}^{(m)} \leftarrow A^{(m)} \odot \sigma(M_A^{(m)})$ 
8:      $\tilde{X} \leftarrow X \odot \sigma(M_X)$ 
9:      $\hat{y}^{(m)} \leftarrow f(\tilde{A}^{(m)}, \tilde{X})$ 
10:  end for
11: Compute  $\mathcal{L}$  by Equation 13
12: Update  $(\{M_A^{(m)}\}, M_X)$  via gradient descent
13: end for
14: return  $\{M_A^{(m)}\}_{m \in \mathcal{M}}, M_X$ 

```

Table 5: Hyperparameters for GNNExplainer.

Hyperparameter	Value
Optimization epochs	100
Optimizer	Adam with lr = 0.1
Prediction loss coefficient (λ_{pred})	1.0
Edge sparsity coefficient (λ_e)	0.005
Feature sparsity coefficient (λ_x)	1.0
Entropy coefficient (λ_{ent})	edge: 1.0; feature: 0.1
Laplacian smoothness coefficient (λ_{lap})	1.0

Algorithm 3 PGM-Explainer under MetaXplain

```

1: Input: Heterogeneous graph  $G$ , trained HeteroGNN  $f$ , meta-path set  $\mathcal{M}$ , target node  $v$ , hops  $k$ , perturbation samples  $n$ 
2: Output: Meta-path-conditioned probabilistic explanations  $\{\mathcal{B}^{(m)}\}_{m \in \mathcal{M}}$ 
3: Extract  $k$ -hop subgraph  $\mathcal{G}(v)$ 
4: for  $m \in \mathcal{M}$  do
5:   Identify node set  $\mathcal{N}_v^{(m)}$ 
6:   Initialize perturbation dataset  $\mathcal{D}^{(m)}$ 
7:   for  $i = 1$  to  $n$  do
8:     Perturb node features in  $\mathcal{N}_v^{(m)}$ 
9:     Evaluate  $f(\mathcal{G}(v))$  with only view  $m$  perturbed
10:    Append perturbation and prediction change to  $\mathcal{D}^{(m)}$ 
11:  end for
12: end for
13: Perform conditional independence tests on  $\{\mathcal{D}^{(m)}\}$ 
14: Select statistically dependent nodes from each meta-path
15: Learn Bayesian network  $\{\mathcal{B}^{(m)}\}$ 
16: return  $\{\mathcal{B}^{(m)}\}_{m \in \mathcal{M}}$ 

```

Table 6: Hyperparameters for PGM-Explainer.

Hyperparameter	Value
Perturbation samples	10
χ^2 threshold	0.05
Prediction drop threshold	0.1
Feature perturbation mode	Binary

D More Information about Extended Algorithms under MetaXplain**D.1 Perturbation-Based Meta-Path Explanations**

PGM-Explainer. Under C1–C2, we apply PGM-Explainer to produce meta-path-specific node importances via randomized perturbations and conditional dependence testing. For each meta-path view m , we collect candidate nodes in the extracted neighborhood and generate binary perturbation samples by randomly perturbing node features (independently per view) and evaluating the predictor. We then compute a χ^2 contingency test between the perturbation state of each candidate node and the perturbation sensitivity of the target node prediction, yielding a p-value per node per view. Finally, we convert p-values into importance weights (smaller p-values \Rightarrow larger weights), producing a node mask vector for each meta-path view.

D.2 Shapley-Style Meta-Path Explanations

Shapley-style explainers treat structural elements as players in a cooperative game. Under C3(B), we compute Shapley attributions conditioned on a single meta-path view while holding the other views fixed.

GNNShap. For a chosen meta-path view m with E_m edges, we define a coalition by a binary vector $\mathbf{z} \in \{0, 1\}^{E_m}$ and form $G^{(m)}(\mathbf{z})$ by removing edges with $z_e = 0$. The value function evaluates the predictor with only view m masked:

$$v_m(\mathbf{z}) = f\left(G_v^{(1)}, \dots, G_v^{(m)}(\mathbf{z}), \dots, G_v^{(M)}; v\right). \quad (18)$$

We then fit a weighted linear surrogate (KernelSHAP-style) over sampled coalitions to estimate edge Shapley values $\{\mathcal{S}_e\}_{e=1}^{E_m}$, producing edge attributions per view.

GraphSVX. GraphSVX defines players as neighboring nodes of v within a fixed meta-path view, samples node coalitions, and fits a KernelSHAP-style linear surrogate to obtain node attributions. In our pipeline, node-level attributions can be optionally lifted to edge scores by assigning each node’s value to its incident edges for comparison against edge-level explainers.

Algorithm 5 GraphSVX under MetaXplain

```

1: Input: Heterogeneous graph  $G$ , trained HeteroGNN  $f$ , meta-path set  $\mathcal{M}$ , target node  $v$ , hops  $k$ , coalition samples  $n$ , size parameter  $S$ 
2: Output: Meta-path-conditioned Shapley values  $\{\mathcal{S}^{(m)}\}_{m \in \mathcal{M}}$ 
3: Extract  $k$ -hop subgraphs  $\mathcal{G}(v)$ 
4: Map target node  $v$  to local index  $v'$ 
5: Compute full prediction  $(p^*, c^*) \leftarrow f(G_v, v')$ 
6: Select relevant feature indices  $\mathcal{F}$ 
7: for  $m \in \mathcal{M}$  do
8:   Identify neighbor set  $\mathcal{N}_v^{(m)}$ 
9:   Determine number of players  $M^{(m)} \leftarrow |\mathcal{N}_v^{(m)}| + |\mathcal{F}|$ 
10:  if  $M^{(m)} \leq 1$  then
11:     $\phi^{(m)} \leftarrow 0$ 
12:    continue
13:  end if
14:  Sample coalition masks  $Z^{(m)} \in \{0, 1\}^{n \times M^{(m)}}$ 
15:  Compute Shapley kernel weights  $\pi^{(m)}$ 
16:  for each coalition  $z_i \in Z^{(m)}$  do
17:    Mask neighbors and features according to  $z_i$ 
18:    Evaluate masked prediction  $f_i^{(m)} \leftarrow f(G_v^{(m)}, z_i)$ 
19:  end for
20:  Fit weighted linear model  $g^{(m)}$  on  $(Z^{(m)}, f^{(m)})$ 
21:  Extract Shapley values  $\mathcal{S}^{(m)}$  from  $g^{(m)}$ 
22: end for
23: return  $\{\mathcal{S}^{(m)}\}_{m \in \mathcal{M}}$ 

```

Algorithm 4 GNNShap under MetaXplain

```

1: Input: Heterogeneous graph  $G$ , trained HeteroGNN  $f$ , meta-path set  $\mathcal{M}$ , target node  $v$ , hops  $k$ , coalition samples  $n$ 
2: Output: Meta-path-conditioned Shapley values  $\{\mathcal{S}\}_{m \in \mathcal{M}}$ 
3: Extract  $k$ -hop subgraphs  $\mathcal{G}(v)$ 
4: Compute full prediction  $(f_{\text{full}}, c^*) \leftarrow f(G_v, v)$ 
5: for  $m \in \mathcal{M}$  do
6:   Let  $E^{(m)} \leftarrow |E(G_v^{(m)})|$ 
7:   if  $E^{(m)} \leq 1$  then
8:      $\phi^{(m)} \leftarrow 0$ 
9:     continue
10:   end if
11:   Build edge-player set  $\mathcal{P}^{(m)} \leftarrow E(G_v^{(m)})$ 
12:   Instantiate sampler  $\mathcal{S}^{(m)}$  with  $|\mathcal{P}^{(m)}|$  players and  $n$  samples
13:   Sample coalition masks  $Z^{(m)}$  and kernel weights  $\pi^{(m)}$ 
14:   Compute null prediction  $f_{\text{null}}^{(m)}$  (meta-path removed)
15:   Compute coalition predictions
16:    $\hat{y}^{(m)} \leftarrow f(\{G_v^{(i)} | i \neq m\}, G_v^{(m)}(z); v)$ 
17:   Select solver:
18:     WLS if  $E^{(m)} \leq 1000$ , else WLR
19:   Solve weighted regression to obtain  $\mathcal{S}^{(m)}$ 
20: end for
21: return  $\{\mathcal{S}^{(m)}\}_{m \in \mathcal{M}}$ 

```

Table 7: Hyperparameters for GNNShap.

Hyperparameter	Value
Coalition samples	15,000
Shapley solver	WLS ($E \leq 1000$), WLR (otherwise)
Ridge regularization	10^{-3}

Table 8: Hyperparameters for GraphSVX.

Hyperparameter	Value
Coalition samples	1000
Maximum coalition size	3
Coalition sampling strategy	SmarterSeparate
Feature marginalization	Expectation
Surrogate model	Weighted Linear Regression
Node-feature balance	nodes only
Multi-class explanation	False

Algorithm 1 Grad under MetaXplain

```

1: Input: Heterogeneous graph  $G$ , trained HeteroGNN  $f$ , meta-path set  $\mathcal{M}$ , target node  $v$ , hops  $k$ 
2: Output: Meta-path-conditioned node importance  $\{I_{\text{Grad}}^{(m)}\}_{m \in \mathcal{M}}$ 
3: Extract  $k$ -hop subgraph  $\mathcal{G}(v)$ 
4: Initialize feature tensors  $\{X^{(m)}\}$  with gradient tracking
5: Compute prediction  $f(v)$  on  $\mathcal{G}(v)$ 
6:  $c^* \leftarrow \arg \max f(v)$ 
7: Compute loss  $\mathcal{L}(v, c^*)$ 
8: for  $m \in \mathcal{M}$  do
9:    $\nabla_{X^{(m)}} \mathcal{L} \leftarrow \partial \mathcal{L} / \partial X^{(m)}$ 
10:   $I_{\text{Grad}}^{(m)}(i) \leftarrow \left\| \partial \mathcal{L} / \partial x_i^{(m)} \right\|_2$ 
11: end for
12: return  $\{I_{\text{Grad}}^{(m)}\}_{m \in \mathcal{M}}$ 

```

E xPath Implementation Details

We set the sampling budget to $m=10$ and the candidate budget to $b=5$ in all experiments.